Unisexual reproduction promotes foraging for mating partners in the global human fungal pathogen *Cryptococcus deneoformans*

Ci Fu, Torin P. Thielhelm, and Joseph Heitman [1]

1 Department of Molecular Genetics and Microbiology, Duke University Medical Center, Durham, NC, 27710, USA

Corresponding author:
Joseph Heitman, MD, PhD
Department of Molecular Genetics and Microbiology
Duke University Medical Center
322 CARL Building Box 3546
Durham, NC 27710, USA
Tel: 919-684-2824
Fax: 919-684-2790
Email: heitm001@duke.edu

Running title: Foraging for mating in *Cryptococcus deneoformans*

Summary

Courtship is an important step towards successful mating in sexual organisms. However, courtship is challenging for the *Cryptococcus neoformans* pathogenic species complex, comprised of opportunistic fungal pathogens, as 99% of isolates are of the α mating type [1, 2]. In the absence of mating partners of the opposite mating type, *C. deneoformans* can undergo unisexual reproduction, during which a yeast-to-hyphal morphological transition occurs [3]. Unisexual hyphal growth is a quantitative trait, which reflects a strain's relative ability to undergo unisexual reproduction [4]. In this study, we determined whether unisexual reproduction confers an ecological benefit by promoting foraging for mating partners. Through competitive mating assays using strains with different ability to undergo unisexual reproduction, this sexual cycle did not enhance competition for mating partners of the same mating type, but when cells of the opposite mating type were present, cells with enhanced unisexual reproduction were more competitive for mating partners of either the same or the opposite mating type. Enhanced mating competition was also observed in a strain with enhanced unisexual reproduction that lacks the mating repressor gene *GPA3*, which encodes a Gα subunit that contributes to pheromone response. We also established that hyphal growth during unisexual reproduction promotes foraging for mating partners through mating confrontation assays. We further showed that in unisexual cells the pheromone response pathway is induced in the presence of cells of the opposite mating type, thereby priming these cells to compete for mating partners. Mating competition also resulted in a fitness cost during growth. Taken

51 together, these findings suggest that in addition to pheromone sensing, *C.*
52 *deneoformans* employs hyphal growth, a physiological tactic, during unisexual
53 reproduction to forage for mating partners at a relatively long distance, which
54 echoes the courtship strategies evolved in other eukaryotic organisms and makes
55 this study the first to describe an intricate two-part courtship behavior in the fungal
56 kingdom.
57

Introduction

Successful courtship is key to the evolutionary success of sexual eukaryotic organisms, and many species have evolved distinct strategies to locate and choose a mating partner. For example, primates and humans utilize aggression to secure a mating partner [5]; male hummingbirds apply acoustic control using tail feathers during high-speed dives to court females [6]; male *Drosophila* vibrate their wings to generate at least three different songs to trigger mating responses in females [7]; male tree-hole frogs also adopt acoustic strategies taking advantage of tree trunk cavities to attract females [8]; and female pipefish display a temporal striped pattern ornament to woo male partners [9]. These examples demonstrate that complex eukaryotic organisms can employ visual, vocal, or mechanical tactics to secure a mate and transmit their genetic traits to the next generation.

In eukaryotic fungal systems, mating often involves a morphological transition. *Saccharomyces cerevisiae* yeast cells undergo polarized growth and form shmoo projections in preparation for cell fusion during mating [10]. In filamentous fungi, including both ascomycetes and basidiomycetes, sexual reproduction involves the formation of a fruiting body (perithecium and basidium, respectively) [11]. In the ascomycetes, *Candida albicans* yeast cells undergo a white-opaque switch to initiate mating [12]. Despite their divergent sexual strategies, these morphological transitions are all controlled by the pheromone response pathway [13]. During yeast mating, physical agglutination of yeast cells

81 does not promote courtship, but rather a gradient of pheromone signals is crucial
82 for successful cell-cell fusion during early mating [14, 15]. Similarly, in
83 *Schizosaccharomyces pombe*, local pheromone signals and a spatially focal
84 pheromone response dictate cell-cell pairing and fusion position during early
85 mating processes [16, 17]. In *C. albicans*, overexpression of pheromone
86 response MAP kinase pathway components can enhance mating efficiency [18].
87 These studies establish that the pheromone response pathway plays a critical
88 role in promoting fungal mating efficiency.

89

90 The opportunistic human fungal pathogen *Cryptococcus deneoformans*
91 undergoes a yeast-to-hyphal morphological transition upon mating induction [19].
92 This species has two modes of sexual reproduction: bisexual reproduction
93 between cells of opposite mating types and unisexual reproduction involving cells
94 of only one mating type [3, 19, 20]. Cell fusion between *MAT***a** and *MAT*α cells
95 during bisexual reproduction, and between two *MAT*α cells during unisexual
96 reproduction, triggers hyphal development [21]. This morphological transition is
97 orchestrated by the pheromone response pathway [21, 22]. However, recent
98 studies have shown that hyphal growth during unisexual reproduction can also
99 occur independent of cell fusion and the pheromone response pathway [23-26],
100 and that pheromone-independent hyphal development is dependent upon the
101 calcineurin pathway [23, 27].

102 Because 99% of identified natural and clinical isolates are of the α mating
103 type, unisexual reproduction likely has significant ecological impacts on the

104 *Cryptococcus* species complex population structure and diversity [1, 2]. The
105 limited abundance of *MAT***a** cells in natural environments restricts outcrossing
106 and in the absence of **a**-α mating, unisexual reproduction has been shown to
107 reverse Muller's rachet and offset the low abundance of *MAT***a** cells to avoid an
108 evolutionary dead end [28]. Unisexual reproduction can also generate genotypic
109 and phenotypic diversity *de novo* [29]. Interestingly, population genetics studies
110 have revealed that genome recombination occurs frequently among
111 environmental isolates [30-32], even those that are exclusively α mating type,
112 providing evidence that unisexual reproduction involving fusion of *MAT*α cells of
113 distinct genotypes allows recombination in nature. Despite these evolutionary
114 benefits, cell fusion-independent solo-unisexual reproduction also occurs and
115 because this pathway involves genetically identical genomes, it does not
116 contribute to genome reshuffling or recombination. Similar to pseudohyphal
117 differentiation in *S. cerevisiae*, *C. deneoformans* unisexual hyphal growth has an
118 ecological benefit in promoting foraging for nutrients and habitat exploration in
119 the surrounding environments [33, 34]. In this study, we address whether
120 unisexual reproduction has an additional ecological benefit in promoting foraging
121 for mating partners, which may facilitate recombination in nature.

122

Results and discussion

Strains with enhanced unisexual reproduction potential are more competitive for mating partners of the opposite mating type

In *C. deneoformans*, hyphal growth is a quantitative trait associated with unisexual reproduction, which is influenced by the mating-type locus α allele [4]. To test whether unisexual reproduction impacts competition for mating partners, we utilized hyphal growth as a determinant of a strain's ability to undergo unisexual reproduction and performed mating competition experiments employing three *MAT*α and three *MAT***a** *C. deneoformans* strains with different degrees of hyphal growth potential (Figure 1A). Among these strains, several were F2 progeny derived from crosses between the environmental *MAT***a** isolate NIH433 and the clinical *MAT*α isolate NIH12 including a high hyphal (HH) strain XL190α, two intermediate hyphal (MH) strains, XL280α and XL187**a**, and a low hyphal (LH) strain JEC20**a** [3, 19, 35-37]. LH strain JEC21α and HH strain XL280**a** are congenic strains of JEC20**a** and XL280α, respectively, derived through 10 rounds of backcrossing (Figure S1) [35, 37, 38]. For each mating competition experiment, cells of different hyphal growth backgrounds carrying dominant, selectable drug resistance markers were mixed, spot-inoculated, and incubated on V8 agar media for 4 days (Figure 1B). Cells were recovered on YPD medium to obtain colony forming units (CFU), and on YPD medium supplemented with different two-drug combinations to determine the cell fusion frequencies. Cell fusion frequencies were compared between different pairs of

145 strains within the same mating mixture to determine whether unisexual
146 reproduction confers benefits in competition for mating partners (Figure 1B).

147 Prior to the mating competition experiments, cell fusion frequencies were
148 compared between different hyphal strains. During unisexual reproduction, the
149 *MAT*α MH strain displayed a significantly higher cell fusion frequency (5 cell
150 fusion events per million CFU) compared to the HH and LH strains (0.013 and
151 0.019 cell fusion events per million CFU, respectively), in which cell fusion rarely
152 occurred (Figure 1C). This suggests that the ability to undergo more unisexual
153 hyphal growth is not strictly correlated with the α-α cell fusion efficiency. In
154 contrast, during bisexual reproduction, unisexual hyphal growth was well
155 correlated with **a**-α cell fusion efficiency. HH strains had a cell fusion frequency
156 (53 cell fusion events per thousand CFU) about 108 times higher than MH
157 strains, which in turn had a cell fusion frequency (0.49 cell fusion events per
158 thousand CFU) about 26 times higher than LH strains (0.019 cell fusion events
159 per thousand CFU) (Figure 1D). In all of the strains tested, **a**-α cell fusion during
160 bisexual reproduction occurred at a much higher level compared to α-α cell
161 fusion during unisexual reproduction, similar to previous findings [3, 26].

162 Cell fusion has been previously shown to be dispensable for solo-
163 unisexual reproduction [22, 26], which can account for the observed poor
164 correlation between hyphal growth and α-α cell fusion frequency. Thus, we
165 hypothesize that unisexual reproduction may not provide an advantage in
166 competing for mating partners of the same mating type. Indeed, when we
167 performed the unisexual mating competition assay using the HH, MH, and LH

168 strains, we observed that HH and LH cells yielded the most fusion products with
169 a cell fusion frequency of 1.3 cell fusion events per million CFU, while MH cells
170 that exhibited the highest cell fusion frequency (Figure 1C) failed to compete
171 against cells of other hyphal backgrounds (Figure 1E), indicating that neither α-α
172 cell fusion frequency nor unisexual hyphal growth can be used to predict mating
173 partner preference, which supports the hypothesis that unisexual reproduction
174 does not promote competition for mating partners during unisexual reproduction.

175 To test whether unisexual reproduction plays a role in competing for
176 mating during bisexual reproduction, mating competition assays were conducted
177 for a given *MAT***a** isolate between two *MAT*α strains of different hyphal growth
178 phenotypes. Interestingly, cells of the higher hyphal strain had a significantly
179 higher cell fusion frequency with *MAT***a** cells compared to cells of the lower
180 hyphal strain (Figure 2A-I). In the presence of HH *MAT***a** cells, HH *MAT*α cells
181 fused with *MAT***a** cells 24 times more efficiently than LH *MAT*α cells (Figure 2A)
182 and 8.1 times more efficiently than MH *MAT*α cells (Figure 2B), and MH *MAT*α
183 cells fused with *MAT***a** cells 5.8 times more efficiently than LH *MAT*α cells (Figure
184 2C). In the presence of MH *MAT***a** cells, HH *MAT*α cells fused with *MAT***a** cells
185 14.5 times more efficiently than LH *MAT*α cells (Figure 2D) and 6.5 times more
186 efficiently than MH *MAT*α cells (Figure 2E), and MH *MAT*α cells fused with *MAT***a**
187 cells 4.6 times more efficiently than LH *MAT*α cells (Figure 2F). In the presence
188 of LH *MAT***a** cells, HH *MAT*α cells fused with *MAT***a** cells 8.9 times more
189 efficiently than LH *MAT*α cells (Figure 2G) and 5.3 times more efficiently than MH
190 *MAT*α cells (Figure 2H), and MH *MAT*α cells fused with *MAT***a** cells 1.7 times

191 more efficiently than LH *MAT*α cells (Figure 2I). Taken together, these results
192 suggest that higher unisexual hyphal growth correlates with competition for
193 mating partners of the opposite mating type during bisexual reproduction. It was
194 also noted that the mating competition advantage decreased for each
195 competition pair (HH vs LH, HH vs MH, and MH vs LH) with the decreasing
196 hyphal phenotype of the *MAT***a** cells (Figure 2ADG, 2BEH, 2CFI), suggesting that
197 increased hyphal growth of *MAT***a** cells can also promote cell fusion.

198 In competition for the HH or MH *MAT***a** cells, the presence of higher
199 hyphal *MAT*α cells promoted **a**-α cell fusion (Figure 2A-F). HH *MAT***a** and HH
200 *MAT*α cells fused at a frequency of 52 cell fusion events per thousand CFU in the
201 presence of MH *MAT*α cells compared to 10 cell fusion events per thousand CFU
202 in the presence of LH *MAT*α cells (5.2-fold) (Figure 2A-B). HH *MAT***a** and MH
203 *MAT*α cells fused at a frequency of 6.4 cell fusion events per thousand CFU in
204 the presence of HH *MAT*α cells compared to 3.4 cell fusion events per thousand
205 CFU in the presence of LH *MAT*α cells (1.9-fold) (Figure 2B-C). Similar trends
206 were observed during competition for MH *MAT***a** cells in that the presence of MH
207 *MAT*α cells increased MH *MAT***a** and HH *MAT*α cell fusion frequency by 4.5-fold
208 compared to the presence of LH *MAT*α cells (Figure 2D-E), and the presence of
209 HH *MAT*α cells increased MH *MAT***a** and MH *MAT*α cell fusion frequency by 2.2-
210 fold compared to the presence of LH *MAT*α cells (Figure 2E-F). However, cell
211 fusion frequencies between *MAT***a** cells and LH *MAT*α cells were comparable in
212 the presence of HH or MH *MAT*α cells (0.41 or 0.59 cell fusion events per
213 thousand CFU for HH *MAT***a** cells, and 0.02 or 0.02 cell fusion events per

214 thousand CFU for MH *MAT***a** cells) (Figure 2A, C, D, F). Interestingly, no
215 enhancement of cell fusion frequency by high hyphal *MAT*α cells was observed
216 during competition for LH *MAT***a** cells (Figure 2G-I). Notably, the enhancement of
217 cell fusion frequency by higher hyphal *MAT*α cells did not occur when either
218 *MAT***a** or *MAT*α LH cells were involved in **a**-α cell fusion, suggesting that strains
219 with poor unisexual reproduction potential have a disadvantage in competing for
220 mating partners during bisexual reproduction.

221

222 Although our results suggest that unisexual reproduction does not
223 correlate with competition for mating partners of the same mating type, we found
224 that better unisexual hyphal growth correlated with higher α-α cell fusion
225 frequency in ménage à trois matings with three partners, including a *MAT***a**
226 partner. In the presence of HH or MH *MAT***a** cells, HH and MH *MAT*α cells fused
227 at higher frequencies (26 and 27 cell fusion events per million CFU, respectively)
228 compared to HH and LH *MAT*α cells (8.1 and 3.4 cell fusion events per million
229 CFU, respectively) (Figure 2J, K), and in the presence of HH, or MH, or LH *MAT***a**
230 cells, HH and LH *MAT*α cells fused at higher frequencies (8.1, 3.4, and 2.8 cell
231 fusion events per million CFU, respectively) compared to MH and LH *MAT*α cells
232 (0.71, 0.28, and 0.14 cell fusion events per million CFU, respectively) (Figure 2K,
233 L), suggesting that unisexual reproduction promotes competition for mating
234 partners of the same mating type in the presence of *MAT***a** cells. We also
235 observed a trend where α-α cell fusion frequencies (HH and MH, HH and LH,
236 and MH and LH) decreased with reduced hyphal *MAT***a** cells (Figure 2J, K, L),

237 suggesting that the unisexual hyphal growth of *MAT***a** cells can further enhance
238 α-α cell fusion. In summary, strains with robust unisexual reproduction compete
239 for mating partners during bisexual reproduction, and during unisexual
240 reproduction in the presence of *MAT***a** cells.

241

242 ***gpa3*Δ mutation enhances competition for mating partners of the same or**
243 **the opposite mating type**

244 The pheromone response pathway plays an important role in the yeast-to-
245 hyphal morphological transition during *C. deneoformans* sexual reproduction.
246 This signaling cascade is controlled by G proteins and RGS proteins, including
247 the Gα protein Gpa3 which represses hyphal growth during mating [39-42]. To
248 further examine the impact of enhanced hyphal growth during mating
249 competition, we generated enhanced hyphal strains by deleting the *GPA3* gene
250 in the LH strain JEC21α. *gpa3*Δ mutants exhibited significantly increased hyphal
251 growth during both unisexual and bisexual reproduction compared to the parental
252 strain (Figure 3A). Next mating competition assays were conducted using the
253 enhanced hyphal strain JEC21α *gpa3*Δ (EH) to test its ability to compete for
254 mating partners.

255

256 Similar to the observation in HH, MH, and LH strains, enhanced unisexual
257 reproduction did not increase cell fusion between *MAT*α cells but did enhance
258 cell fusion frequency by 4-fold between *MAT***a** and *MAT*α cells compared to the

259 parental LH strain (Figure 3B, C). Unisexual mating competition assays were
260 performed to compare the abilities of LH and EH *MAT*α cells to fuse with MH
261 *MAT*α cells. In the control assay, cell fusion frequencies were comparable
262 between cells of all three strain combinations (MH with LH-*NAT*, MH with LH-
263 *NEO*, and LH-*NAT* with LH-*NEO*) (Figure 3D). EH cells fused with MH cells at a
264 significantly higher frequency of 2.8 cell fusion events per million CFU compared
265 to LH cells (85-fold) (Figure 3E), suggesting that enhanced unisexual
266 reproduction increases competitiveness for mating partners of the same mating
267 type. In the mating competition during bisexual reproduction, no advantage was
268 observed in the fusion of LH *MAT***a** cells and either EH or the parental LH *MAT*α
269 cells (Figure 3G). However, a 2.9-fold increase was observed in total **a**-α cell
270 fusion events during mating competitions for LH *MAT***a** cells between EH and LH
271 *MAT*α cells compared to control mating competitions for the same *MAT***a** cells
272 between LH-*NAT* and LH-*NEO MAT*α cells, indicating that enhanced unisexual
273 reproduction allows both EH and LH *MAT*α cells to fuse with *MAT***a** mating
274 partners more efficiently during bisexual reproduction. A 2.9-fold increase was
275 observed in α-α cell fusion between EH and LH *MAT*α cells in the presence of LH
276 *MAT***a** cells compared to cell fusion between LH-*NAT* and LH-*NEO MAT*α cells
277 (Figure 3H), suggesting that in the presence of *MAT***a** cells, *GPA3* deletion-
278 enhanced unisexual reproduction also enhances competition for mating partners
279 of the same mating type. Overall, this analysis of the enhanced hyphal growth
280 strain JEC21α *gpa3*Δ provides additional support for models in which increased
281 hyphal growth enhance competition for mating partners.

282 **Unisexual hyphal growth promotes foraging for mating partners**

283 Unisexual reproduction provides evolutionary and ecological benefits for
284 *C. deneoformans* by generating aneuploid progeny with phenotypic diversity and
285 by promoting habitat exploration through unisexual hyphal growth [29, 34]. Here
286 we further show that unisexual cells have an advantage in competing for mating
287 partners within the same colony. We next further tested whether hyphal growth
288 during unisexual reproduction confers benefits in foraging for mating partners.

289 Both long-term and short-term foraging for mating partner experiments
290 suggested that unisexual hyphal growth promoted foraging for mating. In a six-
291 week mating confrontation experiment, hyphae of different *MAT*α unisexual
292 reproduction backgrounds marked with NEO grew towards the same *MAT***a** cells
293 marked with HYG that were at a distance of 4 mm apart (Figure 4A, B). When
294 competing for either the same *MAT***a** or *MAT*α cells (except LH *MAT*α cells), a
295 significant trend was observed that isolates with more hyphal growth yielded
296 more double drug resistant colonies than isolates with reduced hyphal growth
297 (Figure 4C and Table S4). In a seven-day mini-colony mating experiment,
298 colonies derived from single cells produced hyphae that grew towards adjacent
299 colonies of the opposite mating type (Figure S2A). Similar to the long-term
300 mating confrontation experiment, a significant trend was observed in which
301 isolates with more hyphal growth had an advantage in forming double drug
302 resistant colonies (Figure S2B and Table S5). These results suggest that hyphal
303 growth during unisexual reproduction provides an ecological benefit in promoting
304 foraging for mating partners in adjacent environments.

305

306 **Pheromone response pathway activation is correlated with unisexual**
307 **hyphal growth phenotype during bisexual reproduction**

308 Elevated pheromone response pathway activation and increased
309 response to pheromones are critical to successful courtship during mating in *S.*
310 *cerevisiae* and *C. albicans* [14, 15, 18]. *S. cerevisiae* utilizes the α-factor
311 protease Bar1 and **a**-factor barrier Afb1 to discriminate mating partners with
312 different pheromone levels and drive evolution towards higher pheromone
313 production for efficient mating [43-45]. Pheromones also stimulate mating and
314 the yeast-to-hyphal morphological transition during *C. neoformans* bisexual
315 reproduction [46]. To determine the role of the pheromone response pathway
316 during *C. deneoformans* mating competition, expression levels were examined
317 for the genes encoding the pheromones MFα and MF**a**, the pheromone receptors
318 Ste3α and Ste3**a**, the MAP kinase Cpk1, the transcription factors Mat2 and Znf2,
319 and the plasma membrane fusion protein Prm1 [26, 39, 47].

320 Pheromone response pathway activation did not correlate with the
321 unisexual hyphal growth phenotype in *MAT***a** or *MAT*α strains. In *MAT***a** strains,
322 all of the pheromone response pathway genes were significantly upregulated in
323 the HH strain XL280**a** compared to the MH and LH strains, but only *MF***a** and
324 *PRM1* were significantly upregulated in the MH strain XL187**a** compared to the
325 LH strain JEC20**a** (Figure S3). In *MAT*α strains, all of the pheromone response
326 pathway genes were significantly upregulated in the HH and MH strains
327 compared to the LH strain JEC21α, but the MH strain XL280α had a significantly

328 higher pheromone pathway activation compared to the HH strain XL190α (Figure
329 S3). The pheromone pathway was significantly upregulated in the EH strain
330 JEC21α *gpa3*Δ compared to the parental LH strain JEC21α (Figure S3). These
331 expression analyses suggest that pheromone response pathway activation *per*
332 *se* is not sufficient to explain the ability to undergo unisexual reproduction and its
333 association with competition for mating partners. It was previously shown that the
334 cell fusion protein Prm1 is not required for unisexual reproduction [26], and
335 certain environmental factors, such as copper and glucosamine, can induce
336 hyphal growth independently of the pheromone response pathway [23, 24]. In a
337 recent study on the quorum sensing peptide Qsp1, deletion of pheromone and
338 pheromone receptor genes had little impact on hyphal growth during unisexual
339 reproduction [25], further indicating the polygenic nature of unisexual
340 reproduction.

341 Despite the incongruent association of the pheromone response pathway
342 and the ability to undergo unisexual reproduction, pheromone response pathway
343 activation was correlated with the mating competition for partners of the opposite
344 mating type. The expression patterns of the pheromone response pathway genes
345 matched the hyphal growth phenotype during bisexual reproduction with the
346 exception of the *MF***a** and *CPK1* genes (Figure 5A). Although *MF***a** expression
347 was lower in HH strains compared to MH strains during bisexual reproduction,
348 the significant upregulation of the *MF*α and pheromone receptor genes *STE3*α
349 and *STE3***a** may compensate for the overall pheromone response activation
350 (Figure 5A). The poor correlation between *CPK1* expression and hyphal growth

351 may be due to post-translational control of the MAP kinase through
352 phosphorylation, which can relieve a requirement for expression level
353 upregulation during pathway activation. The largely congruent association of
354 pheromone response pathway activation and unisexual hyphal growth phenotype
355 suggests that in the presence of cells of the opposite mating type, unisexual cells
356 have an advantage by priming the pheromone response pathway in both *MAT***a**
357 and *MAT*α cells to compete for mating partners.

358

359 **Enhanced unisexual reproduction resulted in a fitness cost**

360 Upregulation of the pheromone response pathway enhances mating
361 efficiency; however, this upregulation can result in a fitness cost in *S. cerevisiae*
362 and *C. albicans* [18, 48]. In yeast, a short-term experimental evolution
363 experiment showed that mutations abrogating expression of 23 genes involved in
364 mating conferred a fitness benefit during yeast growth when functions of these
365 genes are not required [48]. In *C. albicans*, cells undergo a white-opaque switch
366 and upregulate the pheromone response pathway, which results in a fitness cost
367 for the opaque cells [18]. Considering that the pheromone response pathway is
368 activated at a higher level in *C. deneoformans* strains with more hyphal growth
369 during bisexual reproduction, we investigated whether unisexual reproduction
370 confers a fitness cost.

371 Growth curve analyses in YPD liquid medium were performed using an
372 automated Tecan Sunrise absorbance reader to determine the fitness of different

373 unisexual strains. The cultures were agitated with vigorous shaking for one
374 minute bihourly before each OD_{600} measurement. The minimum agitation allows
375 for differentiation of growth curve kinetics among the strains tested, which would
376 otherwise be indistinguishable when grown on solid YPD medium. Compared to
377 the low hyphal growth strains JEC21α and JEC20**a**, *gpa3*Δ mutants exhibited a
378 growth defect in nutrient rich media, suggesting that enhanced unisexual
379 reproduction resulted in a fitness tradeoff (Figure S4). Interestingly, deletion of
380 the *GPA3* gene in the sister species *C. neoformans* did not enhance unisexual
381 reproduction or cause a growth defect compared to the non-unisexual strain
382 KN99**a** (Figure S4). It has been shown that the pheromone response pathway
383 activation by *GPA3* gene deletion is lower in KN99**a** than in JEC21 or JEC20,
384 indicating that deletion of *GPA3* is not sufficient to rewire cellular responses to
385 induce unisexual reproduction in *C. neoformans* [39].

386 We next performed fitness competition experiments. After 10 days of
387 incubation on YPD agar medium, the EH strain (92%) outcompeted the parental
388 LH strain (8%), whereas after 10 days of incubation on mating-inducing V8 agar
389 medium, the LH strain (85%) outcompeted EH strain (15%) (Figure 5B). This
390 suggested there was no tradeoff in fitness cost in EH cells when unisexual
391 reproduction was not induced, but upon induction of hyphal growth under mating-
392 inducing conditions, pheromone response pathway activation resulted in a fitness
393 cost. We performed an additional fitness competition and observed that, in the
394 presence of *MAT***a** cells, the fitness advantage of EH cells (92% without vs 36%
395 with *MAT***a** cells) on YPD agar medium was alleviated (Figure 5C), indicating that

396 a *MAT***a** cell-induced pheromone response may confer a fitness cost upon EH
397 cells. In the presence of *MAT***a** cells on V8 agar medium, enhanced unisexual
398 reproduction (12%) resulted in a similar fitness cost to the competition on V8
399 agar medium without *MAT***a** cells (Figure 5). These fitness competition assays
400 demonstrate that unisexual reproduction results in a fitness cost under mating-
401 inducing conditions or in the presence of opposite mating type partners, which is
402 likely due to the energy cost in the expression of the pheromone response
403 pathway genes. It has been reported that long-term passage on rich media in the
404 lab often diminishes the hyphal growth phenotype of *MAT***a** strains, which further
405 suggests that there is a fitness cost associated with unisexual reproduction [49].
406 Interestingly, in *S. cerevisiae*, the [*SWI*$^{+}$] prion state promotes outcrossing
407 efficiency due to a defect in *HO* expression and mating type switching, which
408 also leads to a fitness cost [50]. Taken together, fungal species have evolved
409 different strategies in foraging for mating partners in nature accompanied with a
410 fitness tradeoff.

411 **Conclusion**

412 Sexual reproduction plays a pivotal role in shaping fungal population
413 structure and diversity in nature. However, studies on how fungi secure a mating
414 partner in nature for successful mating are limited. In this study, we aimed to
415 characterize the ecological and evolutionary benefits of unisexual reproduction in
416 *C. deneoformans*. Similar to the landmark study by Jackson and Hartwell
417 showing that higher pheromone production promotes courtship in *S. cerevisiae*
418 [15], we showed that strains with higher potential in unisexual reproduction do
419 not compete for mating partners of the same mating type, but when cells of the
420 opposite mating type are present, unisexual cells upregulate the pheromone
421 response pathway in both *MAT***a** and *MAT*α cells and prime themselves to
422 compete for mating partners of both the same and opposite mating types (Figure
423 6). More interestingly, in addition to pheromone response pathway activation,
424 unisexual cells employ hyphal growth, a physiological tactic, to forage for mating
425 partners at a relatively long distance, which echoes the courtship strategies
426 evolved in other eukaryotic organisms and makes this study the first to describe
427 an intricate two-part courtship behavior in the fungal kingdom. However, this
428 courtship behavior results in a fitness cost for the unisexual cells during mitotic
429 growth under mating inducing conditions.

430 The strains involved in this study were all derived from natural and clinical
431 isolates, suggesting that the ability to undergo unisexual reproduction is likely to
432 span a broad range in the environment. Over 99% of natural and clinical isolates
433 of the *Cryptococcus* species complex are found to be of the α mating type [1, 2].

434 But there is genomic and genetic evidence indicating that recombination is
435 prevalent among these environmental isolates, which underscores that mating
436 occurs in nature [30-32]. We hypothesize that in the presence of *MAT***a** cells
437 sparsely distributed in the environment, unisexual *MAT*α cells are primed for
438 mating, and when rare contacts with *MAT***a** cells do occur, unisexual hyphal
439 growth enables foraging for mating partners. Overall unisexual reproduction can
440 enhance mating competition and promote outcrossing, which provides an
441 evolutionary advantage by promoting genome reshuffling via meiotic
442 recombination.

443 **Materials and methods**

444 **Strains, media, and growth conditions**

445 Strains used in this study are listed in Table S1. Strains with different
446 hyphal growth phenotypes, XL190α, XL280α, JEC21α, XL280**a**, XL187**a**, and
447 JEC20**a**, were selected to represent high, intermediate, and low hyphal strains [3,
448 4, 37, 38]. Yeast cells were grown at 30°C on Yeast extract Peptone Dextrose
449 (YPD) medium. Strains harboring dominant selectable markers were grown on
450 YPD medium supplemented with 100 μg/mL noureothricin (NAT), 200 μg/mL
451 G418 (NEO), or 200 μg/mL hygromycin (HYG) for selection. Mating assays were
452 performed on 5% V8 juice agar medium (pH = 7.0) or Murashige and Skoog (MS)
453 medium minus sucrose (Sigma-Aldrich) in the dark at room temperature for the
454 designated time period.

455

456 **Drug resistant marker strain generation and gene deletion**

457 NAT (pAI3) or NEO (pJAF1) resistant expression constructs were
458 introduced into XL190α, XL280α, and JEC21α, and a HYG (pJAF15) resistant
459 expression construct was introduced into XL280α, XL280**a**, XL187**a**, and JEC20**a**
460 ectopically via biolistic transformation as previously described [51-53].

461 To generate deletion mutants for *GPA3*, a deletion construct consisting of
462 the 5' upstream and 3' downstream regions of *GPA3* gene flanking the *NEO*
463 cassette was generated by overlap PCR as previously described [54]. The *GPA3*
464 deletion construct was introduced into the strain JEC21α via biolistic

465 transformation. Transformants were selected on YPD medium supplemented
466 with G418, and gene replacement by homologous recombination was confirmed
467 by PCR. Primers used to generate these deletion constructs are listed in Table
468 S2.

469

470 **Microscopy**

471 Cells were grown on V8 agar medium for seven days or three weeks in
472 the dark at room temperature to allow hyphal formation. Hyphal growth on the
473 edge of mating patches was imaged using a Nikon Eclipse E400 microscope
474 equipped with a Nikon DXM1200F camera.

475

476 **Competitive mating assays**

477 For each competitive mating assay, cells were grown overnight in YPD
478 liquid medium at 30°C and adjusted to OD_{600}=0.5 in sterile H_2O, and then equal
479 volumes of cells marked with different dominant drug resistant markers were
480 mixed and spot inoculated (50 µl) on V8 agar medium. The mating plates were
481 incubated for four days in the dark at room temperature. The cells were
482 harvested and plated in serial dilution on YPD medium and YPD medium
483 supplemented with different two drug combinations (NAT and NEO, NAT and
484 HYG, or NEO and HYG). The cells were incubated for three to five days at room
485 temperature and colony forming units were counted. Cell fusion frequencies were
486 determined as double drug resistant CFU/total CFU. The complete competitive

487 mating experimental design is listed in Table S3. Each mating competition was
488 performed in biological triplicate.

489

490 **Foraging for mating assays**

491 To investigate whether unisexual hyphal growth enables cells foraging for
492 mating partners, we performed long-term confrontation and short-term mini-
493 colony mating experiments. For the confrontation mating experiment, HYG
494 resistant XL280**a**, XL187**a**, and JEC20**a** were streaked and grown on V8 medium
495 to form a line of cells, and then NEO resistant XL190α, XL280α, and JEC21α,
496 and JEC21α *gpa3*Δ::*NEO* were spot inoculated 4 mm apart in parallel along the
497 *MAT***a** cells. Unisexual hyphae grew towards cells of the opposite mating type for
498 six weeks. Then the cells were collected and plated on YPD medium
499 supplemented with HYG and NEO. After incubation at room temperature for
500 three to five days, total double drug resistant colony forming units were counted
501 to determine whether unisexual hyphal growth confers an advantage in foraging
502 for mating partners. Each confrontation mating experiment was performed in
503 biological quintuplicate. For the mini-colony mating experiment, cells of above
504 mentioned HYG resistant *MAT***a** strains and NEO resistant *MAT*α strains were
505 grown overnight in YPD liquid medium and adjusted to OD_{600}=0.008. For each
506 mating pair, 100 µl of *MAT***a** cells and 100 µl of *MAT*α cells were mixed and
507 plated on V8 agar medium to form evenly spaced mini colonies. Unisexual
508 hyphae grew towards adjacent hyphae for seven days. Then the cells were
509 collected and plated on YPD medium and YPD medium supplemented with HYG

510 and NEO. The cells were incubated for three to five days at room temperature
511 and colony forming units were counted. Cell fusion frequencies were determined
512 as double drug resistant CFU/total CFU. Each mating was performed in
513 biological triplicate.

514

515 **RNA extraction and qRT-PCR**

516 To examine pheromone response pathway activation, qRT PCR
517 experiments were performed on RNA extracted from cells incubated on V8 agar
518 medium for 36 hours as previously described [26]. In brief, XL190α, XL280α,
519 JEC21α, JEC21α *gpa3*Δ::*NEO*, XL280**a**, XL187**a**, and JEC20**a** were grown
520 overnight in YPD liquid medium and adjusted to OD_{600}=2 in sterile H_2O. Then
521 cells of individual strains and an equal-volume mixtures of cells for crosses
522 between XL190α and XL280**a**, XL280α and XL187**a**, JEC21α and JEC20**a**, and
523 JEC21α *gpa3*Δ::*NEO* and JEC20**a** were spotted (250 µl) on V8 medium and
524 incubated for 36 hours. Cell patches were harvested and flash frozen in liquid
525 nitrogen. RNA was extracted using TRIzol reagent (Thermo) following the
526 manufacturer's instructions. RNA was treated with Turbo DNAse (Ambion), and
527 single-stranded cDNA was synthesized by AffinityScript RT-RNAse (Stratagene).
528 cDNA synthesized without the RT/RNAse block enzyme mixture was used to
529 control for genomic DNA contamination. The relative expression levels of
530 targeted genes were measured by qRT PCR using Brilliant III ultra-fast SYBR
531 green QPCR mix (Stratagene) in an Applied Biosystems 7500 Real-Time PCR
532 system. A "no template control" was used to analyze the resulting melting curves

533 to exclude primer artifacts for each target gene. Gene expression levels were
534 normalized to the endogenous reference gene *GPD1* using the comparative
535 ΔΔCt method. Primers used for qRT-PCR are listed in Table S2. For each target
536 gene and each sample, technical triplicate and biological triplicate were
537 performed.

538

539 **Fitness competition and growth curve assays**

540 Competition experiments were performed to compare fitness between low
541 and enhanced hyphal strains. Overnight cultures of JEC21α *NAT*, JEC21α
542 *gpa3*Δ::*NEO*, and XL280**a** were washed with H_2O twice and cell densities were
543 determined with a hemocytometer. For each competition experiment, 10 μl of
544 H_2O containing 100,000 cells of each strain was spotted on either YPD or V8
545 agar medium and incubated in the dark at room temperature for 10 days. Cells
546 were collected and plated on YPD medium supplemented with NAT or G418 to
547 determine colony forming units. Cell mixtures were plated before incubation to
548 control for equal mixing. Each competition was performed in triplicate. Fitness
549 was determined by calculating the percentile of the recovered CFU of each strain
550 out of the total recovered dominant drug resistant CFU.

551 To determine the growth fitness of different unisexual strains, KN99**a**,
552 KN99**a** *gpa3*Δ::*NEO*, JEC20**a**, JEC20**a** *gpa3*Δ::*NEO*, JEC21α, and JEC21α
553 *gpa3*Δ::*NEO* were grown overnight in YPD liquid medium and washed twice in
554 H_2O. 10,000 cells for each strain were resuspended in 200 μl YPD liquid medium

555 and incubated in a 96-well plate (Corning) at 30°C with vigorous shaking for 1
556 min bihourly. OD_{600} readings were measured bi-hourly after shaking using an
557 automated Tecan Sunrise absorbance reader. Each sample was tested in
558 quintuplicate.

559

560 **Statistical analysis**

561 All statistical analyses were performed using the Graphpad Prism 7
562 program. Welch's t-test was performed for each pairwise comparison, and one-
563 way ANOVA was performed for each group analysis with a *p* value lower than
564 0.05 considered statistically significant (* indicates $0.01<p\leq0.05$, ** indicates
565 $0.001<p\leq0.01$, *** indicates $0.0001<p\leq0.001$, and **** indicates $p\leq0.0001$).

Acknowledgements

We thank Daniel Lew, Sheng Sun, Zanetta Chang, and Shelby Priest for critical reading of the manuscript. This work was supported by NIH/NIAID R37 grant AI39115-21 and R01 grant AI50113-15 to J.H.

571 **Author Contributions**

572 Conceptualization, F.C., T.T.P., and H.J.; Formal analysis, F.C., T.T.P.,
573 and H.J.; Funding acquisition, H.J; Investigation, F.C. and T.T.P.; Methodology,
574 F.C., T.T.P., and H.J.; Resources, F.C. and H.J.; Supervision, H.J.; Writing –
575 original draft, F.C.; Writing – review & editing, F.C., T.T.P., and H.J.

576

577 **Declaration of Interests**

578 The authors declare no competing interests.

579

580 ## References

581

582 1. Litvintseva, A.P., Kestenbaum, L., Vilgalys, R., and Mitchell, T.G. (2005). Comparative
583 analysis of environmental and clinical populations of *Cryptococcus neoformans*. J. Clin.
584 Microbiol. *43*, 556-564.
585 2. Kwon-Chung, K.J., and Bennett, J.E. (1978). Distribution of α and **a** mating types of
586 *Cryptococcus neoformans* among natural and clinical isolates. Am. J. Epidemiol *108*, 337-
587 340.
588 3. Lin, X., Hull, C.M., and Heitman, J. (2005). Sexual reproduction between partners of the
589 same mating type in *Cryptococcus neoformans*. Nature *434*, 1017-1021.
590 4. Lin, X., Huang, J.C., Mitchell, T.G., and Heitman, J. (2006). Virulence attributes and
591 hyphal growth of *C. neoformans* are quantitative traits and the *MAT*α allele enhances
592 filamentation. PLoS Genet. *2*, e187.
593 5. Muller, M.N., and Wrangham, R.W. (2009). Sexual coercion in primates and humans: an
594 evolutionary perspective on male aggression against females, (Cambridge, Mass.:
595 Harvard University Press).
596 6. Clark, C.J., and Mistick, E.A. (2018). Strategic acoustic control of a hummingbird
597 courtship dive. Curr Biol *28*, 1257-1264.
598 7. Clemens, J., Coen, P., Roemschied, F.A., Pereira, T.D., Mazumder, D., Aldarondo, D.E.,
599 Pacheco, D.A., and Murthy, M. (2018). Discovery of a new song mode in *Drosophila*
600 reveals hidden structure in the sensory and neural drivers of behavior. Curr Biol *28*,
601 2400-2412 e2406.
602 8. Lardner, B., and bin Lakim, M. (2002). Animal communication: tree-hole frogs exploit
603 resonance effects. Nature *420*, 475.
604 9. Berglund, A., and Rosenqvist, G. (2001). Male pipefish prefer ornamented females. Anim
605 Behav *61*, 345-350.
606 10. Ydenberg, C.A., and Rose, M.D. (2008). Yeast mating: a model system for studying cell
607 and nuclear fusion. Methods Mol. Biol. *475*, 3-20.
608 11. Dyer, P.S., Ingram, D.S., and Johnstone, K. (1992). The control of sexual morphogenesis
609 in the ascomycotina. Biol Rev *67*, 421-458.
610 12. Miller, M.G., and Johnson, A.D. (2002). White-opaque switching in *Candida albicans* is
611 controlled by mating-type locus homeodomain proteins and allows efficient mating. Cell
612 *110*, 293-302.
613 13. Jones, S.K., Jr., and Bennett, R.J. (2011). Fungal mating pheromones: choreographing the
614 dating game. Fungal Genet. Biol. *48*, 668-676.
615 14. Jackson, C.L., and Hartwell, L.H. (1990). Courtship in *Saccharomyces cerevisiae*: an early
616 cell-cell interaction during mating. Mol. Cell Biol. *10*, 2202-2213.
617 15. Jackson, C.L., and Hartwell, L.H. (1990). Courtship in *S. cerevisiae*: both cell types choose
618 mating partners by responding to the strongest pheromone signal. Cell *63*, 1039-1051.
619 16. Dudin, O., Merlini, L., and Martin, S.G. (2016). Spatial focalization of pheromone/MAPK
620 signaling triggers commitment to cell-cell fusion. Genes Dev. *30*, 2226-2239.
621 17. Merlini, L., Khalili, B., Bendezu, F.O., Hurwitz, D., Vincenzetti, V., Vavylonis, D., and
622 Martin, S.G. (2016). Local pheromone release from dynamic polarity sites underlies cell-
623 cell pairing during yeast mating. Curr Biol. *26*, 1117-1125.

624 18. Scaduto, C.M., Kabrawala, S., Thomson, G.J., Scheving, W., Ly, A., Anderson, M.Z.,
625 Whiteway, M., and Bennett, R.J. (2017). Epigenetic control of pheromone MAPK
626 signaling determines sexual fecundity in *Candida albicans*. Proc. Natl. Acad. Sci. USA
627 *114*, 13780-13785.
628 19. Kwon-Chung, K.J. (1976). Morphogenesis of *Filobasidiella neoformans*, the sexual state
629 of *Cryptococcus neoformans*. Mycologia *68*, 821-833.
630 20. Wickes, B.L., Mayorga, M.E., Edman, U., and Edman, J.C. (1996). Dimorphism and
631 haploid fruiting in *Cryptococcus neoformans*: association with the α-mating type. Proc.
632 Natl. Acad. Sci. USA *93*, 7327-7331.
633 21. Fu, C., Sun, S., Billmyre, R.B., Roach, K.C., and Heitman, J. (2015). Unisexual versus
634 bisexual mating in *Cryptococcus neoformans*: Consequences and biological impacts.
635 Fungal Genet. Biol. *78*, 65-75.
636 22. Wang, L., and Lin, X. (2011). Mechanisms of unisexual mating in *Cryptococcus*
637 *neoformans*. Fungal Genet. Biol. *48*, 651-660.
638 23. Gyawali, R., Zhao, Y., Lin, J., Fan, Y., Xu, X., Upadhyay, S., and Lin, X. (2017). Pheromone
639 independent unisexual development in *Cryptococcus neoformans*. PLoS Genet. *13*,
640 e1006772.
641 24. Xu, X., Lin, J., Zhao, Y., Kirkman, E., So, Y.S., Bahn, Y.S., and Lin, X. (2017). Glucosamine
642 stimulates pheromone-independent dimorphic transition in *Cryptococcus neoformans*
643 by promoting Crz1 nuclear translocation. PLoS Genet *13*, e1006982.
644 25. Tian, X., He, G.-J., Hu, P., Chen, L., Tao, C., Cui, Y.-L., Shen, L., Ke, W., Xu, H., Zhao, Y., et
645 al. (2018). *Cryptococcus neoformans* sexual reproduction is controlled by a quorum
646 sensing peptide. Nat. Microbiol. *3*, 698-707.
647 26. Fu, C., and Heitman, J. (2017). *PRM1* and *KAR5* function in cell-cell fusion and karyogamy
648 to drive distinct bisexual and unisexual cycles in the *Cryptococcus* pathogenic species
649 complex. PLoS Genet. *13*, e1007113.
650 27. Fu, C., Donadio, N., Cardenas, M.E., and Heitman, J. (2018). Dissecting the roles of the
651 calcineurin pathway in unisexual reproduction, stress responses, and virulence in
652 *Cryptococcus deneoformans*. Genetics *208*, 639-653.
653 28. Roach, K.C., and Heitman, J. (2014). Unisexual reproduction reverses Muller's ratchet.
654 Genetics *198*, 1059-1069.
655 29. Ni, M., Feretzaki, M., Li, W., Floyd-Averette, A., Mieczkowski, P., Dietrich, F.S., and
656 Heitman, J. (2013). Unisexual and heterosexual meiotic reproduction generate
657 aneuploidy and phenotypic diversity *de novo* in the yeast *Cryptococcus neoformans*.
658 PLoS Biol. *11*, e1001653.
659 30. Saul, N., Krockenberger, M., and Carter, D. (2008). Evidence of recombination in mixed-
660 mating-type and alpha-only populations of *Cryptococcus gattii* sourced from single
661 eucalyptus tree hollows. Eukaryot. Cell *7*, 727-734.
662 31. Litvintseva, A.P., Marra, R.E., Nielsen, K., Heitman, J., Vilgalys, R., and Mitchell, T.G.
663 (2003). Evidence of sexual recombination among *Cryptococcus neoformans* serotype A
664 isolates in Sub-Saharan Africa. Eukaryot. Cell *2*, 1162-1168.
665 32. Campbell, L.T., Currie, B.J., Krockenberger, M., Malik, R., Meyer, W., Heitman, J., and
666 Carter, D. (2005). Clonality and recombination in genetically differentiated subgroups of
667 *Cryptococcus gattii*. Eukaryot. Cell *4*, 1403-1409.
668 33. Cullen, P.J., and Sprague, G.F., Jr. (2012). The regulation of filamentous growth in yeast.
669 Genetics *190*, 23-49.

670 34. Phadke, S.S., Feretzaki, M., and Heitman, J. (2013). Unisexual reproduction enhances
671 fungal competitiveness by promoting habitat exploration via hyphal growth and
672 sporulation. Eukaryot. Cell *12*, 1155-1159.
673 35. Heitman, J., Allen, B., Alspaugh, J.A., and Kwon-Chung, K.J. (1999). On the origins of
674 congenic MATalpha and MAT**a** strains of the pathogenic yeast *Cryptococcus*
675 *neoformans*. Fungal Genet Biol *28*, 1-5.
676 36. Kwon-Chung, K.J. (1975). A new genus, *Filobasidiella*, the perfect state of *Cryptococcus*
677 *neoformans*. Mycologia *67*, 1197-1200.
678 37. Kwon-Chung, K.J., Edman, J.C., and Wickes, B.L. (1992). Genetic association of mating
679 types and virulence in *Cryptococcus neoformans*. Infect. Immun. *60*, 602-605.
680 38. Zhai, B., Zhu, P., Foyle, D., Upadhyay, S., Idnurm, A., and Lin, X. (2013). Congenic strains
681 of the filamentous form of *Cryptococcus neoformans* for studies of fungal
682 morphogenesis and virulence. Infect. Immun. *81*, 2626-2637.
683 39. Hsueh, Y.P., Xue, C., and Heitman, J. (2007). G protein signaling governing cell fate
684 decisions involves opposing Gα subunits in *Cryptococcus neoformans*. Mol. Biol. Cell *18*,
685 3237-3249.
686 40. Gong, J., Grodsky, J.D., Zhang, Z., and Wang, P. (2014). A Ric8/synembryn homolog
687 promotes Gpa1 and Gpa2 activation to respectively regulate cyclic AMP and pheromone
688 signaling in *Cryptococcus neoformans*. Eukaryot Cell *13*, 1290-1299.
689 41. Feretzaki, M., and Heitman, J. (2013). Genetic circuits that govern bisexual and unisexual
690 reproduction in *Cryptococcus neoformans*. PLoS Genet. *9*, e1003688.
691 42. Nielsen, K., Cox, G.M., Wang, P., Toffaletti, D.L., Perfect, J.R., and Heitman, J. (2003).
692 Sexual cycle of *Cryptococcus neoformans* var. *grubii* and virulence of congenic **a** and α
693 isolates. Infect. Immun. *71*, 4831-4841.
694 43. Huberman, L.B., and Murray, A.W. (2013). Genetically engineered transvestites reveal
695 novel mating genes in budding yeast. Genetics *195*, 1277-1290.
696 44. Sprague, G.F., Jr., and Herskowitz, I. (1981). Control of yeast cell type by the mating type
697 locus. I. Identification and control of expression of the **a**-specific gene *BAR1*. J. Mol. Biol.
698 *153*, 305-321.
699 45. Banderas, A., Koltai, M., Anders, A., and Sourjik, V. (2016). Sensory input attenuation
700 allows predictive sexual response in yeast. Nat Commun *7*, 12590.
701 46. Shen, W.C., Davidson, R.C., Cox, G.M., and Heitman, J. (2002). Pheromones stimulate
702 mating and differentiation via paracrine and autocrine signaling in *Cryptococcus*
703 *neoformans*. Eukaryot. Cell *1*, 366-377.
704 47. Lin, X., Jackson, J.C., Feretzaki, M., Xue, C., and Heitman, J. (2010). Transcription factors
705 Mat2 and Znf2 operate cellular circuits orchestrating opposite- and same-sex mating in
706 *Cryptococcus neoformans*. PLoS Genet. *6*, e1000953.
707 48. Lang, G.I., Murray, A.W., and Botstein, D. (2009). The cost of gene expression underlies a
708 fitness trade-off in yeast. Proc. Natl. Acad. Sci. USA *106*, 5755-5760.
709 49. Tscharke, R.L., Lazera, M., Chang, Y.C., Wickes, B.L., and Kwon-Chung, K.J. (2003).
710 Haploid fruiting in *Cryptococcus neoformans* is not mating type α-specific. Fungal Genet.
711 Biol. *39*, 230-237.
712 50. Newby, G.A., and Lindquist, S. (2017). Pioneer cells established by the [*SWI*$^{+}$] prion can
713 promote dispersal and out-crossing in yeast. PLoS Biol *15*, e2003476.
714 51. Fraser, J.A., Subaran, R.L., Nichols, C.B., and Heitman, J. (2003). Recapitulation of the
715 sexual cycle of the primary fungal pathogen *Cryptococcus neoformans* var. *gattii*:
716 implications for an outbreak on Vancouver Island, Canada. Eukaryot. Cell *2*, 1036-1045.

717 52. Idnurm, A., Reedy, J.L., Nussbaum, J.C., and Heitman, J. (2004). *Cryptococcus*
718 *neoformans* virulence gene discovery through insertional mutagenesis. Eukaryot. Cell *3*,
719 420-429.
720 53. Davidson, R.C., Cruz, M.C., Sia, R.A., Allen, B., Alspaugh, J.A., and Heitman, J. (2000).
721 Gene disruption by biolistic transformation in serotype D strains of *Cryptococcus*
722 *neoformans*. Fungal Genet. Biol. *29*, 38-48.
723 54. Davidson, R.C., Blankenship, J.R., Kraus, P.R., de Jesus Berrios, M., Hull, C.M., D'Souza,
724 C., Wang, P., and Heitman, J. (2002). A PCR-based strategy to generate integrative
725 targeting alleles with large regions of homology. Microbiology *148*, 2607-2615.

726

727

728 **Figure legends**

729

730 **Figure 1. Unisexual reproduction does not enhance competition for mating**
731 **partners of the same mating type.**

732 (A) Hyphal growth on V8 agar medium for three weeks of high (HH), intermediate
733 (MH), and low (LH) hyphal *MAT*α and *MAT***a** strains. The scale bar represents
734 500 μm. (B) Experimental design of the unisexual and bisexual mating
735 competition. (C-E) Average cell fusion frequencies. Error bars indicate standard
736 deviation. (C) Unisexual α-α cell fusion frequencies of high, intermediate, and low
737 hyphal strains. (D) Bisexual **a**-α cell fusion frequencies of high, intermediate, and
738 low hyphal strains. (* indicates $0.01<p\leq0.05$ and ** indicates $0.001<p\leq0.01$ for
739 each pairwise comparison) (E) Cell fusion frequencies among three *MAT*α strains
740 of different hyphal growth phenotypes during unisexual mating competition are
741 shown.

742

743 **Figure 2. Unisexual reproduction enhances competition for mating partners**
744 **of both mating types in a and α mixed populations.**

745 (A-C) Cell fusion frequencies are shown during mating competition for a high
746 hyphal *MAT***a** strain between high and low hyphal *MAT*α strains (A), high and
747 intermediate hyphal *MAT*α strains (B), and intermediate and low hyphal *MAT*α
748 strains (C). (D-F) Cell fusion frequencies are depicted during mating competition
749 for an intermediate hyphal *MAT***a** strain between high and low hyphal *MAT*α

750 strains (D), high and intermediate hyphal *MAT*α strains (E), and intermediate and
751 low hyphal *MAT*α strains (F). (G-I) Cell fusion frequencies during mating
752 competition for a low hyphal *MAT***a** strain between high and low hyphal *MAT*α
753 strains (G), high and intermediate hyphal *MAT*α strains (H), and intermediate and
754 low hyphal *MAT*α strains (I). (A-I) * indicates 0.01<*p*≤0.05, ** indicates
755 0.001<*p*≤0.01, and *** indicates 0.0001<p≤0.001 for each pairwise comparison.
756 (J-L) Unisexual α-α cell fusion frequencies between high and intermediate hyphal
757 *MAT*α strains (J), high and low hyphal *MAT*α strains (K), and intermediate and
758 low hyphal *MAT*α strains (L) in presence of *MAT***a** strains of different hyphal
759 growth phenotypes. ** indicates 0.001<*p*≤0.01, *** indicates 0.0001<p≤0.001,
760 and **** indicates p≤0.0001 for each group analysis by one-way ANOVA.

761

762 **Figure 3. *gpa3*Δ mutation-enhances unisexual reproduction and**
763 **competition for mating partners of both the same and opposite mating**
764 **types.**

765 (A) Hyphal growth on V8 agar medium for one week for enhanced hyphal strain
766 (JEC21α *gpa3*Δ::*NEO*) during unisexual (top) and unilateral bisexual (bottom)
767 development compared to low hyphal strain (JEC21α). The scale bar represents
768 500 μm. (B-C) Unisexual α-α (B) and bisexual **a**-α (C) cell fusion frequencies
769 between two low hyphal strains and between low and enhanced hyphal strains.
770 (D-E) Cell fusion frequencies during unisexual mating competition among two low
771 and one intermediate hyphal *MAT*α strains (D), and one low, one enhanced, and

772 one intermediate hyphal *MAT*α strains (E). (F-G) Cell fusion frequencies during
773 bisexual mating competition for a low hyphal *MAT***a** strain between two low
774 hyphal *MAT*α strains (F), and between one low and one enhanced hyphal *MAT*α
775 strain (G). (H) Unisexual α-α cell fusion frequencies between two low hyphal
776 *MAT*α strains, and between one low and one enhanced hyphal *MAT*α strain in
777 the presence of a low hyphal *MAT***a** strain. * indicates 0.01<p≤0.05 for the
778 pairwise comparison.

779

780 **Figure 4. Unisexual development promotes foraging for mating partners in**
781 **a mating confrontation assay.**

782 (A) LH, MH, HH, and EH *MAT*α hyphal cells were grown towards LH, MH, and
783 HH *MAT***a** cells for six weeks. The scale bar represents 500 μm. (B) Schematic
784 diagram for the confrontation mating experiment setup. *MAT***a** cells were grown
785 to form a line of cells, and *MAT*α cells were spot inoculated 4 mm apart in parallel
786 along the *MAT***a** cells. (C) Total G418/HYG resistant colonies produced by each
787 confrontation mating pair. LH, MH, HH, and EH *MAT*α hyphal cells yielded an
788 average of 0.4, 10, 44, and 1.8 double drug resistant colonies with LF *MAT***a**
789 cells, 0.4, 26, 81, and 0.4 double drug resistant colonies with MF *MAT***a** cells, 17,
790 239, 613, and 422 double drug resistant colonies with HF *MAT***a** cells,
791 respectively. * indicates 0.01<p≤0.05, ** indicates 0.001<p≤0.01, and ****
792 indicates p≤0.0001 for each group analysis by one-way ANOVA.

793

794 **Figure 5. Pheromone response pathway activation associated with**
795 **unisexual reproduction confers a fitness cost under mating inducing**
796 **conditions.**

797 (A) Pheromone response pathway activation during bisexual reproduction is
798 correlated with unisexual hyphal growth phenotype. Gene expression patterns for
799 *MF*α, *MF***a**, *STE3*α, *STE3***a**, *CPK1*, *MAT2*, *ZNF2*, and *PRM1* were examined by
800 qRT PCR (* indicates 0.01<*p*≤0.05, ** indicates 0.001<*p*≤0.01, *** indicates
801 0.0001<p≤0.001, and **** indicates p≤0.0001 for each pairwise comparison.).
802 Crosses between high hyphal *MAT***a** (XL280**a**) and *MAT*α (XL190α) strains,
803 between intermediate hyphal *MAT***a** (XL187**a**) and *MAT*α (XL280α) strains,
804 between low hyphal *MAT***a** (JEC20**a**) and *MAT*α (JEC21α) strains, and between
805 low hyphal *MAT***a** (JEC20**a**) and enhanced hyphal *MAT*α (JEC21α *gpa3*Δ::*NEO*)
806 strains were grown on V8 agar medium for 36 hours. The expression levels of
807 genes from the cross between low hyphal strains JEC20**a** and JEC21α were set
808 to 1, and the remaining values were normalized to this. The error bars represent
809 the standard deviation of the mean for three biological replicates. (B-C)
810 Enhanced unisexual reproduction confers a fitness cost under mating-inducing
811 conditions. (B) Equal numbers of cells of a low hyphal strain (JEC21α *NEO*) and
812 an enhanced hyphal strain (JEC21α *gpa3*Δ::*NEO*), and (C) equal numbers of
813 cells of a low hyphal strain (JEC21α *NEO*), an enhanced hyphal strain (JEC21α
814 *gpa3*Δ::*NEO*), and a high hyphal **a** strain (XL280**a**) were co-cultured on YPD and
815 V8 agar medium. CFUs of each strain were counted before plating and after 10
816 days of incubation to determine competition fitness.

817

818 **Figure 6. Model for the role of unisexual reproduction in foraging for**

819 **mating partners.**

820 In the absence of the opposite mating type, unisexual reproduction does not

821 promote foraging for mating partners of the same mating type (left). In the

822 presence of the opposite mating type, unisexual reproduction promotes foraging

823 for mating partners of both the same and the opposite mating type (right). NH: no

824 hyphal growth; LH: low hyphal growth; MH: medium hyphal growth; HH: high

825 hyphal growth.

826 **Supporting information**

827 **Figure S1. Derivation of the strains used in this study.**

828 B4478 *MAT*α, JEC20**a**, XL187**a**, XL190α, and XL280α are F2 progeny from the
829 cross between F1 progeny B3502 *MAT***a** and B3501 *MAT*α, which were derived
830 from a cross between the environmental isolate NIH433 *MAT***a** and the clinical
831 isolate NIH12 *MAT*α. JEC20**a** was then crossed with B4478 *MAT*α, and an α
832 progeny was backcrossed with JEC20**a**. This process was repeated 10 times to
833 yield the congenic partner B4500 JEC21α of B4476 JEC20**a**. XL280α was
834 crossed with JEC20**a**, and an **a** progeny was backcrossed with XL280α. This
835 process was repeated 10 times to yield the congenic partner XL280**a**.

836

837 **Figure S2. Unisexual hyphal growth promotes foraging for mating partners**
838 **in a mini-colony mating assay.**

839 (A) LH, MH, HH, and EH *MAT*α colonies derived from single cells were grown for
840 seven days and in some cases, hyphae were produced towards the LH, MH, and
841 HH *MAT***a** colonies. The scale bar represents 500 μm. (B) Cell fusion frequencies
842 between *MAT***a** and *MAT*α mating partners for each mating pair are shown. *
843 indicates $0.01<p\leq0.05$ and ** indicates $0.001<p\leq0.01$ for each group analysis by
844 one-way ANOVA.

845

846

847 **Figure S3. Pheromone response pathway activation is not correlated with**
848 **unisexual hyphal growth phenotype.**

849 Gene expression patterns for *MF*α, *MF***a**, *STE3*α, *STE3***a**, *CPK1*, *MAT2*, *ZNF2*,
850 and *PRM1* were examined by qRT PCR (* indicates 0.01<*p*≤0.05, ** indicates
851 0.001<*p*≤0.01, *** indicates 0.0001<p≤0.001, and **** indicates p≤0.0001 for
852 each pairwise comparison.). High hyphal *MAT***a** (XL280**a**) and *MAT*α (XL190α)
853 strains, intermediate hyphal *MAT***a** (XL187**a**) and *MAT*α (XL280α) strains, low
854 hyphal *MAT***a** (JEC20**a**) and *MAT*α (JEC21α) strains, and an enhanced hyphal
855 *MAT*α (JEC21α *gpa3*Δ::*NEO*) strain were grown on V8 agar medium for 36
856 hours. The expression levels of low hyphal strain JEC20**a** or JEC21α were set to
857 1, and the remaining values of the same mating type strains were normalized to
858 this. The error bars represent the standard deviation of the mean for three
859 biological replicates.

860

861 **Figure S4. Enhanced unisexual reproduction results in a fitness cost**
862 **during vegetative growth.**

863 Hyphal growth on MS medium for two weeks for *C. neoformans* strains KN99**a**,
864 KN99**a** *gpa3*Δ::*NEO* #1, and KN99**a** *gpa3*Δ::*NEO* #2, and low unisexual and
865 enhanced unisexual *C. deneoformans* strains JEC20**a**, JEC21α, JEC20**a**
866 *gpa3*Δ::*ADE2 ade2*, and JEC21α *gpa3*Δ::*NEO*. The scale bar represents 500 μm.
867 Growth curves were generated using an automated Tecan Sunrise absorbance
868 reader bi-hourly for 72 hours.

869 **Table S1. Strains and plasmids used in this study.**

870 **Table S2. Primers used in this study.**

871 **Table S3. Mating competition experimental design.**

872 **Table S4. p-Values of one-way ANOVA analyses and Welch's t-test for each**
873 **pairwise comparison for the foraging for mating assay during mating**
874 **confrontation.**

875 **Table S5. p-Values of one-way ANOVA analyses and Welch's t-test for each**
876 **pairwise comparison for the foraging for mating assay during mating**
877 **among mini-colonies.**

878

879 **Figure 1**

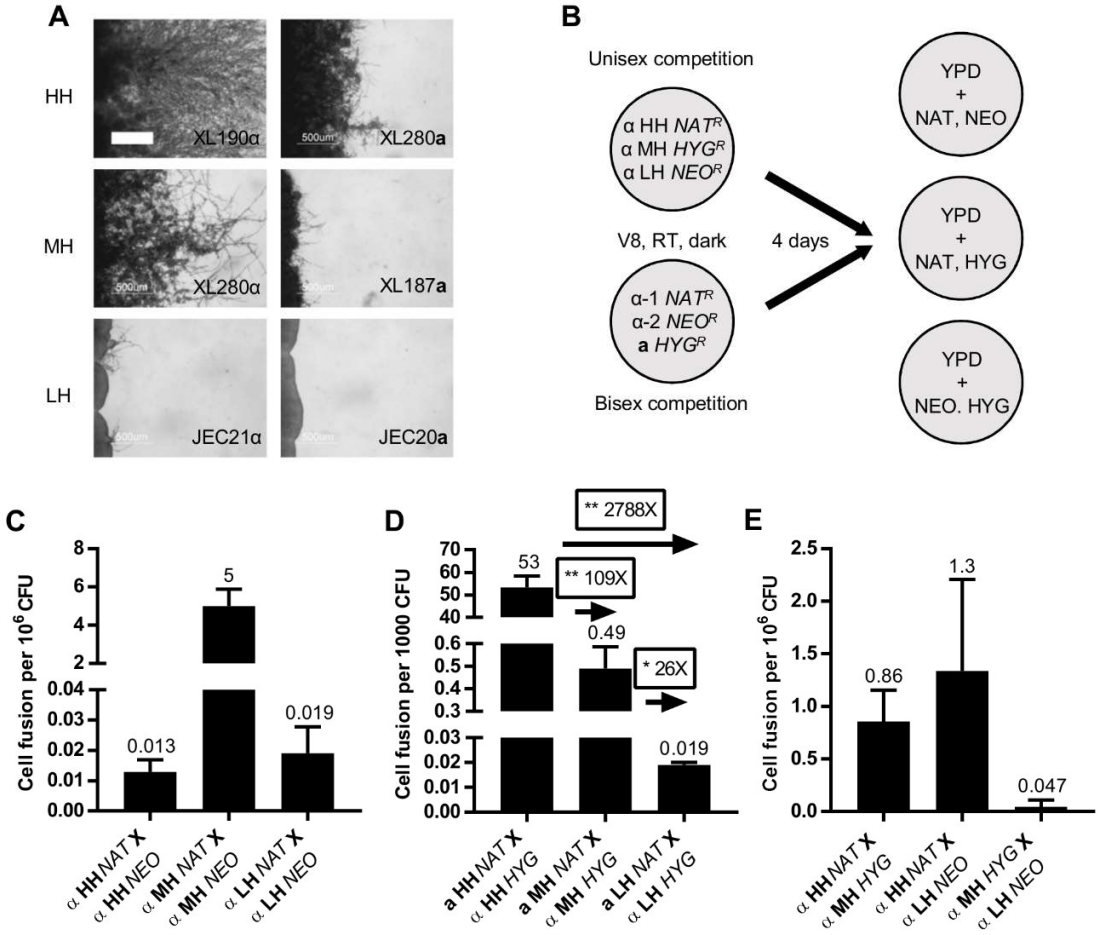

880

881 **Figure 2**

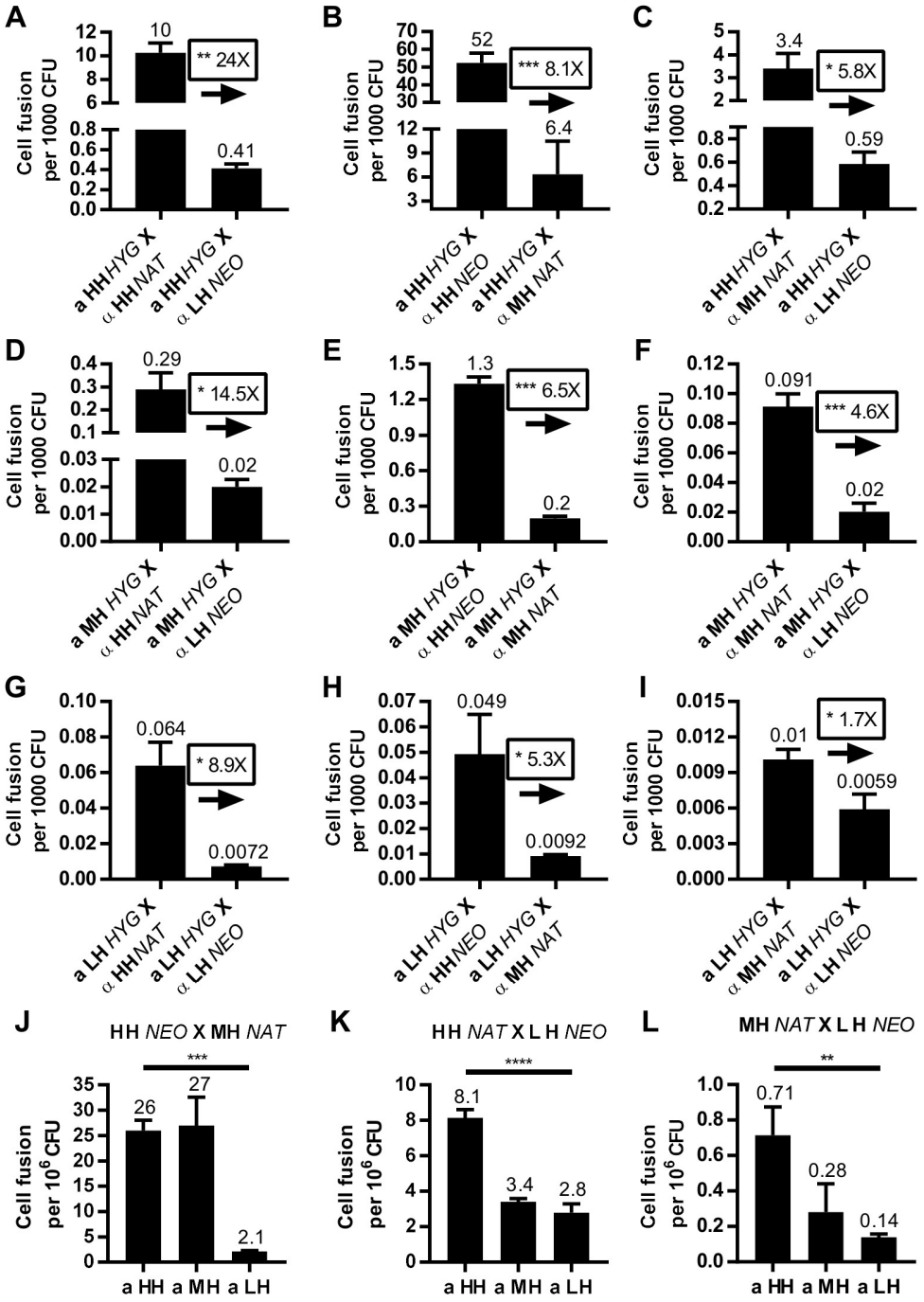

882

883 **Figure 3**

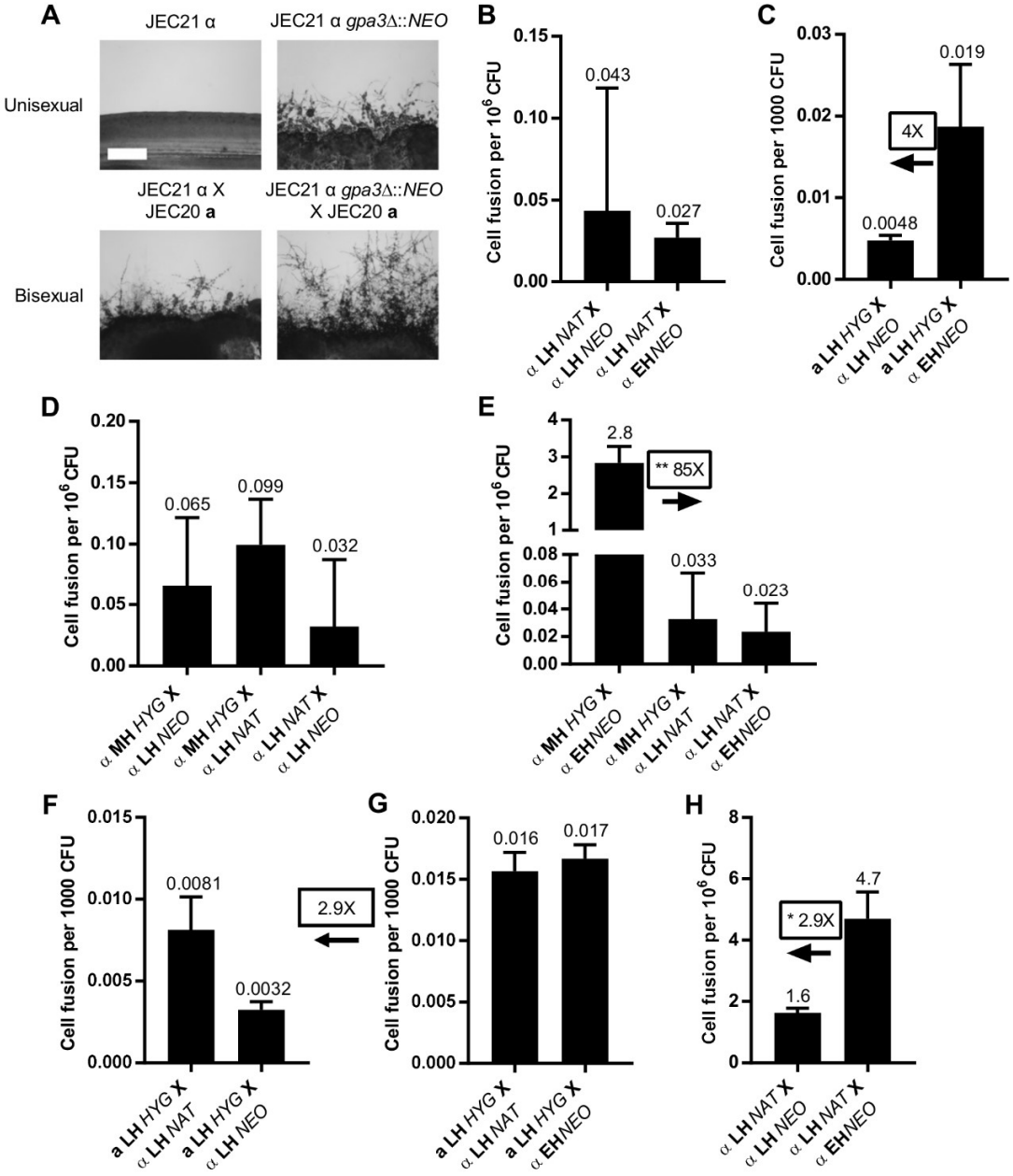

884

885 **Figure 4**

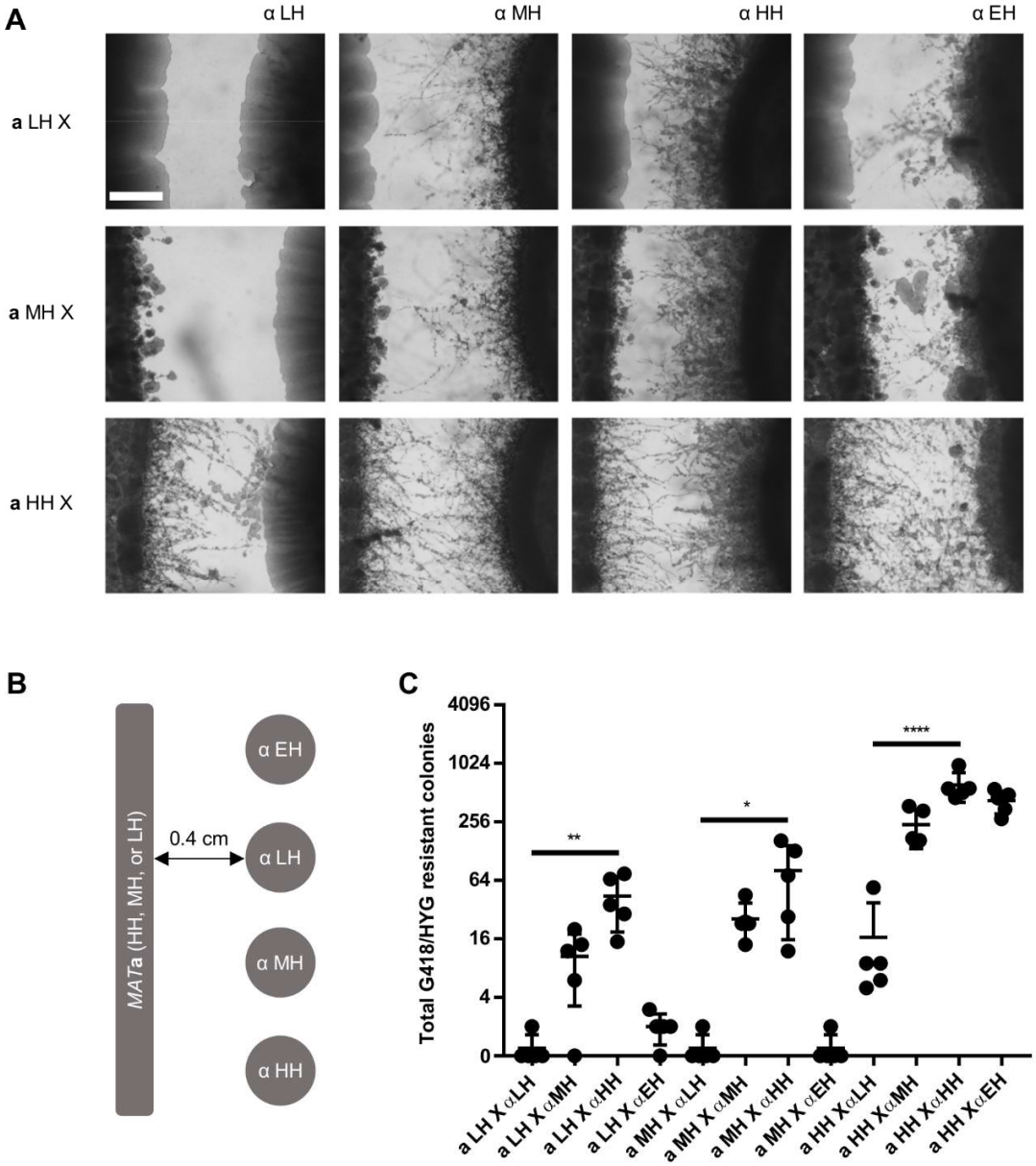

886

887 **Figure 5**

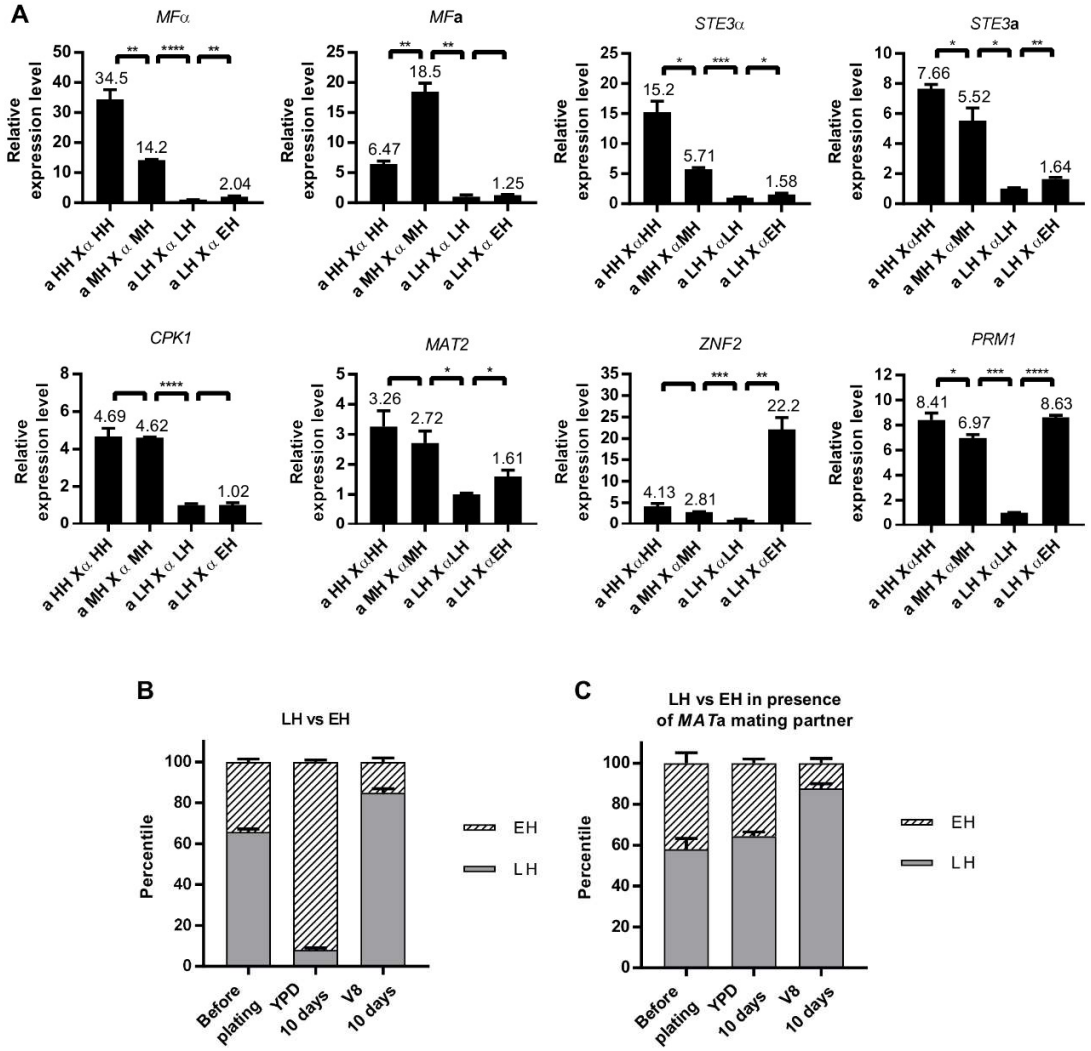

888

889 **Figure 6**

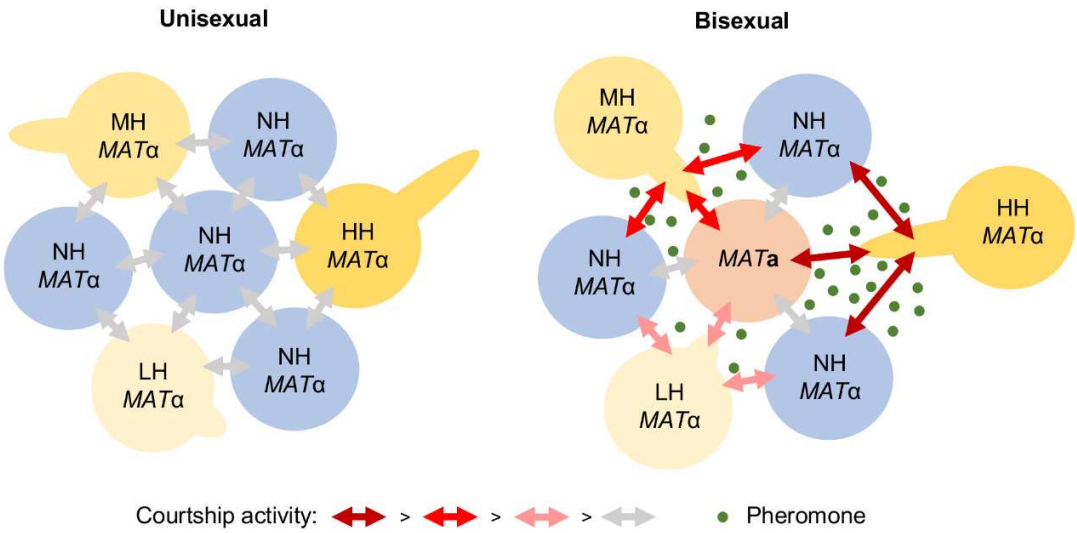

890